

Benzooxadiazole-Based D–A–D Co-Oligomers: Synthesis and Electropolymerization

Palas Baran Pati, Soumyajit Das, Sanjio S. Zade

Department of Chemical Sciences, Indian Institute of Science Education and Research, Kolkata,
P.O. BCKV Campus Main Office, Mohanpur, Nadia, West Bengal 741252, India
Correspondence to: S. S. Zade (E-mail: sanjiozade@iiserkol.ac.in)

Received 31 March 2012; accepted 15 May 2012; published online

DOI: 10.1002/pola.26195

ABSTRACT: Four D–A–D type co-oligomers have been synthesized by Stille condensation between monostannyl derivatives of furan/thiophene/selenophene/3,4-ethylenedioxythiophene (EDOT) and 4,7-dibromo-benzo[1,2,5]oxadiazole. All these co-oligomers were successfully electrochemically polymerized in dichloromethane and characterized by spectroelectrochemistry. All four polymers possess narrow optical band gap. Spectroelectrochemical studies of polymer films on indium tin oxide revealed that the replacement of donor EDOT with furan/thiophene/selenophene has affected the low-energy charge-carrier

(bipolaron) formation significantly. Kinetic studies based on chronoamperometry show that the polymer **P5** (EDOT-capped benzo[1,2,5]oxadiazole system) possess better electrochromic property with high transmittance (66%) in visible region than the other copolymers. © 2012 Wiley Periodicals, Inc. *J Polym Sci Part A: Polym Chem* 000: 000–000, 2012

KEYWORDS: benzooxadiazole; conducting polymers; conjugated polymers; EDOT; electrochromic materials; electropolymerization; oligomers; spectroelectrochemistry; thin films

INTRODUCTION Planarity with an efficient conjugation in organic materials plays important role in achieving low band gap, high conductivity, high mobility, and good electro-optical response. Thiophene-containing π -conjugated systems have received considerable attention for the development of organic electronic devices, such as light-emitting diodes, field-effect transistors, and solar cells because of their good environmental and thermal stability.¹ 3,4-Ethylenedioxythiophene (EDOT) is one of the most important examples of thiophene derivatives both academically and industrially, because the polymers derived from EDOT and its derivatives provide highly conducting and especially stable doped states, a range of optical properties with electronic band gaps varying across the entire visible spectrum, and enhanced redox properties, making them useful for numerous electronic devices.^{2–5} Although thiophene-containing π -conjugated systems are heavily explored, their selenium counterparts have lately drawn decent attention as a novel class of π -conjugated materials exhibiting promising optoelectronic properties⁶ ranging from high conductivity⁷ to high hole mobility.^{8,9} Just by a mere change of sulfur for less electronegative and more polarizable selenium (atomistic approach), one can easily tune the band gap, and thus the optical and electronic properties.^{10–13} Additionally, selenophene system is more vulnerable to electrophilic substitution than its thiophene counterpart.¹⁴ While polythiophene and polyselenophene were

studied, in comparison, polyfuran is almost unnoticed, as the synthesis of polyfuran by direct electrolysis of furan is difficult (>3 V vs. SCE).¹⁵ Recent discoveries on oligofuran¹⁶ proved the potential of furan-based conjugated systems as promising hole transporting material¹⁷ and efficient low band gap polymers for solar cells.^{18,19} The development of furan-based conjugated systems relies on its enhanced solution processability. Compared to sulfur/selenium-based organic electronic materials, oxygen-based materials are more biodegradable¹⁷ and biocompatible which is desirable as, in general, organic electronic materials are not biodegradable and extensive usage of these compounds may generate a significant amount of hazardous waste.^{20,21}

The donor–acceptor (D–A) concept for band gap reduction was first proposed in 1992,²² and since then this strategy was well developed to synthesize small band gap (1.0 eV $< E_g < 1.9$ eV) polymers.²³ By constructing a conjugated chain of alternating donor and acceptor units, the valence and conduction bands could be broadened, which may result in a narrow band gap polymers. This D–A strategy was extensively studied with electron-deficient systems like benzo[1,2,5]thiadiazole (BDT),²⁴ benzo[1,2,5]selenadiazole (BDS),²⁵ and benzo[1,2,5]triazole (BTaz).²⁶ However, their oxygen counterpart, benzo[1,2,5]oxadiazole (BDO), had received limited attention until lately.^{27–31} The exciting report by Toppare and coworkers²⁴ on EDOT-capped BDT

Additional Supporting Information may be found in the online version of this article.

© 2012 Wiley Periodicals, Inc.

system and the report by Cihaner and Algi²⁵ on thiophene/EDOT-capped BDS systems inspired us to explore the D-A polymers based on BDO as acceptor.³¹ Oxygen over sulfur or selenium has more electronegativity; hence, it is possible to stabilize the highest occupied molecular orbital (HOMO) level of the polymers by introducing oxygen containing heterocyclic systems into polymers instead of sulfur or selenium analogs. Thus, replacement of the BTaz, BDT, or BDS with the more electronegative BDO acceptor may result in a polymer with more stabilized HOMO level,^{27,28} which may be beneficial in increasing the efficiency of polymer solar cell while maintaining good solubility and planarity of resulting polymer backbone.^{29,30} Herein, we report the synthesis of furan, thiophene, selenophene, and EDOT-capped BDO co-oligomers anticipating that these would reveal efficient optical and redox properties as a new type of polymer electrochromics when polymerized electrochemically.³¹ The experimental results are also supported by theoretical calculations.

EXPERIMENTAL

All reactions were performed under nitrogen atmosphere to maintain the dry condition. Dry toluene and THF were distilled from sodium/benzophenone prior to use. Anhydrous dichloromethane (DCM), furan, thiophene, selenophene, EDOT, tributyltinchloride (SnBu₃Cl), Pd(PPh₃)₄, tetrabutylammonium perchlorate (TBAPC), and *o*-nitroaniline were purchased from Aldrich and used without further purification. *n*-BuLi (1.6 M solution in hexane) was purchased from Neo-Synth. Tributyl(furan-2-yl)stannane,³² tributyl(thiophen-2-yl)stannane,³³ tributyl(selenophen-2-yl)stannane,³⁴ and tributyl(3,5-ethylenedioxythiophen-2-yl)stannane³⁵ were synthesized according to previously described methods. All the new compounds were characterized by ¹H NMR, ¹³C NMR, and HRMS. ¹H NMR and ¹³C NMR spectra of the compounds were taken on Bruker Avance 500 MHz and Jeol ECS 400 MHz spectrometer with either CDCl₃ or DMSO-*d*₆ as the solvent, and chemical shifts (δ) are reported in parts per million (ppm) relative to tetramethylsilane as the internal standard. Electrochemical studies were carried out with a Princeton Applied Research 263A potentiostat using platinum (Pt) disk electrode as the working electrode, a platinum wire as counter electrode, and an AgCl-coated Ag wire, which was directly dipped in the electrolyte solution, as the reference electrode. Nonaqueous Ag/AgCl wire was prepared by dipping silver wire in a solution of FeCl₃ and HCl. Pt disk electrodes were polished with alumina, water, and acetone and were dried with nitrogen gas before use to remove any incipient oxygen. The electrolyte used was 0.1 M TBAPC in DCM. Electropolymerization was done on indium tin oxide (ITO)-coated glass as a working electrode. The polymer films were deposited on ITO-coated glass electrode with dimensions of 5 × 0.7 cm² at monomer's first oxidation potential (V) versus Ag/AgCl and a passing charge of 50–100 mC in 0.1 M TBAPC/DCM. Before examining the optical properties of polymer films, the films were rinsed with DCM. UV-vis-near infrared (NIR) spectra were recorded on a

HITACHI U-4100 UV-vis-NIR spectrophotometer. In spectrochemical measurements, the working electrode was an ITO-coated glass slide, the counter electrode was a platinum wire, and nonaqueous Ag/AgCl was used as the reference electrode. All electrochemical potentials were reported against Ag/AgCl taking ferrocene as external standard, the $E_{1/2}^{\text{ferrocene}}$ is +0.35 V.

Synthesis of 4,7-Dibromo-benzo[1,2,5]oxadiazole (1)

4,7-Benzo[1,2,5]oxadiazole was prepared starting from *o*-nitroaniline following a literature procedure.³⁶ Diazotization of *o*-nitroaniline (4.14 g, 30 mmol) by silica-sulfuric acid followed by addition of sodium azide afforded the azide derivative (Supporting Information, Scheme S1). Cyclocondensation of the azide derivative in boiling toluene gave benzofuroxane which on treatment with triethylphosphite under reflux condition in ethanol medium resulted deoxygenation to produce BDO.³⁷ Bromination of BDO in the presence of iron powder leads to 4,7-dibromo-benzo[1,2,5]oxadiazole (2 g, overall yield 25%).³⁸ ¹H NMR (400 MHz, CDCl₃, δ , ppm): 7.51 (s, 1H).

General Synthesis of 4a, 4b, 4c, and 5

4,7-Bibromo-benzo[1,2,5]oxadiazole (0.5 mmol) and the corresponding monostannyl derivative (1.0 mmol), that is, tributyl(furan-2-yl)stannane (**2a**)/tributyl(thiophen-2-yl)stannane (**2b**)/tributyl(selenophen-2-yl)stannane (**2c**)/tributyl(3,4-ethylenedioxythiophen-2-yl)stannane (**3**), were dissolved in dry toluene (30 mL), and the solution was purged with nitrogen for 15 min. Pd(PPh₃)₄ (0.05 mmol) was added at room temperature under argon atmosphere. The mixture was stirred at 100 °C for 24 h, cooled, and solvent was evaporated on the rotary evaporator. The residue was subjected to column chromatography to isolate the desired compound.

Compound 4a

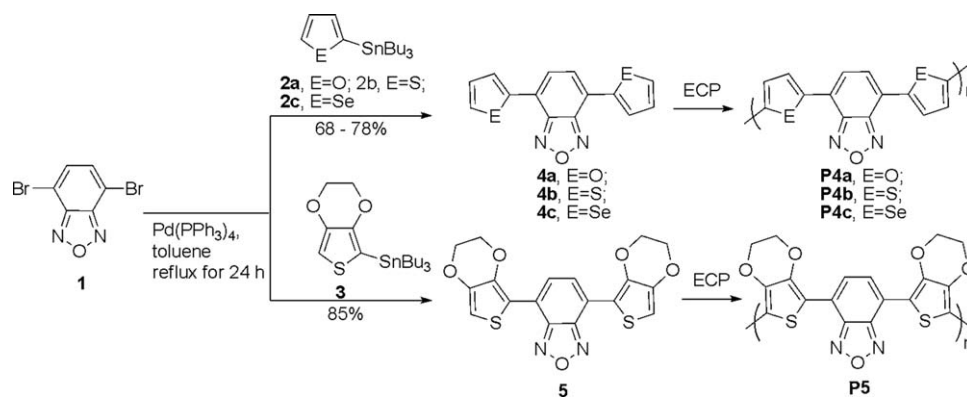
After purification by column chromatography (hexane), pure product was obtained as yellow solid in 72% yield. mp: 118–122 °C. ¹H NMR (500 MHz, DMSO-*d*₆, δ , ppm): 6.78 (m, 1H), 7.38 (d, *J* = 3.5 Hz, 1H), 7.89 (s, 1H), 7.99 (m, 1H). ¹³C NMR (125 MHz, DMSO-*d*₆, δ , ppm): 112.62, 113.04, 116.48, 124.97, 145.14, 146.09, 147.83. HRMS (*m/z*): calcd for C₁₄H₈N₂O₃, 252.0535; found, 252.0541 [M]⁺.

Compound 4b

After purification by column chromatography (DCM:hexane, 1:20), pure product was obtained as orange-yellow solid in 68% yield. mp: 123–125 °C. ¹H NMR (400 MHz, DMSO-*d*₆, δ , ppm): 6.78 (m, 1H), 7.45 (d, *J* = 3.5 Hz, 1H), 7.62 (s, 1H), 8.12 (m, 1H). ¹³C NMR (100 MHz, DMSO-*d*₆, δ , ppm): 112.07, 126.36, 128.62, 128.72, 137.87, 147.84. HRMS (*m/z*): calcd for C₁₄H₈N₂OSe₂, 284.0078; found, 284.0065 [M]⁺.

Compound 4c

After purification by column chromatography (DCM:hexane, 1:20), pure product was obtained as orange-yellow solid in 78% yield. mp: 145–148 °C. ¹H NMR (500 MHz, DMSO-*d*₆, δ , ppm): 7.5 (m, 1H), 7.89 (s, 1H), 8.25 (m, 1H), 8.43 (m, 1H). ¹³C NMR (125 MHz, DMSO-*d*₆, δ , ppm): 112.76, 127.89, 129.99, 130.87, 135.15, 142.25, 147.49. HRMS (*m/z*): calcd for C₁₄H₈N₂OSe₂, 379.8967; found, 379.8963 [M]⁺.



SCHEME 1 Synthetic route to furan, thiophene, selenophene, and EDOT-capped 2,1,3-benzooxadiazole based D–A–D type copolymers.

Compound 5

After purification by column chromatography (ethyl acetate:hexane, 1:10) pure product was obtained as red solid in 85% yield. ^1H NMR (400 MHz, $\text{DMSO-}d_6$, δ , ppm): 4.32 (d, 2H), 4.43 (d, 2H), 6.95 (s, 1H), 8.19 (s, 1H). ^{13}C NMR (100 MHz, $\text{DMSO-}d_6$, δ , ppm): 64.06, 65.18, 103.10, 110.78, 118.42, 127.32, 141.22, 141.79, 147.16. HRMS (m/z): calcd for $\text{C}_{18}\text{H}_{12}\text{N}_2\text{O}_5\text{S}_2$, 400.0188; found, 400.0193 $[\text{M}]^+$.

RESULTS AND DISCUSSION

Synthesis

To demonstrate the effect of the donor and acceptor units on the structure–property relationships four different BDO-based D–A–D co-oligomers, **4a**, **4b**, **4c**, and **5** were studied. Synthesis of **4a**, **4b**, **4c**, and **5** was accomplished by Stille coupling between stannyl derivative of donor (furan, thiophene, selenophene, and EDOT) and 4,7-dibromo-benzo[2,1,3]oxadiazole **1** in toluene medium as shown in Scheme 1.³¹ The selenophene analog **4c** revealed stronger intermolecular interactions (including Se/Se interactions) than their furan (**4a**) or thiophene (**4b**) counterparts, as evidenced by its significantly higher melting point. All the co-oligomers were fully characterized by ^1H NMR, ^{13}C NMR, and high resolution mass spectroscopy analysis.

Electrochemistry and Polymerization

Electrochemical synthesis of conducting polymers offers many advantages over chemical synthesis including the *in situ* deposition of the polymer at the electrode surface and, hence, eliminating processability problems. Cyclic voltammetry experiment on **4a** [Fig. 1(a)], **4b** [Fig. 1(c)], **4c** [Fig. 1(e)], and **5** [Fig. 1(g)] in DCM/TBAPC solvent/electrolyte couple indicated irreversible cyclic voltammograms revealing their first oxidation potentials at 1.2, 1.32, 1.22, and 0.95 V, respectively. The EDOT-based co-oligomer **5** showed the lowest oxidation potential among the four BDO-based co-oligomers, which may be credited to the more electron-rich nature of EDOT. Replacing BTaz, BDT, and BDS with BDO makes it more difficult to extract an electron from the D–A–D systems **4a**, **4b**, **4c**, and **5** resulting in higher first oxidation potential that could be attributed to the higher electron-acceptance nature of BDO stabilizing the HOMO.^{24–26}

Under repeated CV cycles, these D–A–D co-oligomers have undergone smooth polymerization to produce insoluble D–A copolymer deposit at the surface of the platinum working electrode. Meanwhile, an increase in the current intensity was observed, which is due to an increase in the active area of the working electrode owing to electroactive polymer (**P4a**, **P4b**, **P4c**, and **P5**) coating on the Pt electrode (Fig. 1). The inset pictures show the scan rate dependence of the current response during redox cycling of **P4a** [Fig. 1(b)], **P4b** [Fig. 1(d)], **P4c** [Fig. 1(f)], and **P5** [Fig. 1(h)] as a function of different scan rates. It is evident that both the anodic and cathodic peak currents scale linearly with increasing scan rate, which is as expected for an electrode-supported nondiffusive electroactive film.

Electrochemical measurements are important for evaluation of HOMO and lowest unoccupied molecular orbital (LUMO) energy levels. The onset oxidation potential ($E_{\text{onset}}^{\text{ox}}$) of the polymers increases in the order **P5** (-0.18 V) < **P4a** (0.43 V) < **P4b** (0.60 V) < **P4c** (0.78 V), and the HOMO of the polymers **P4a**, **P4b**, **P4c**, and **P5** are calculated as -4.88 , -5.05 , -5.23 , and -4.27 eV, respectively.³⁹ Similar to previous observation,²⁶ we found that HOMO of D–A type copolymer comprising furan as donor is more destabilized than their thiophene or selenophene counterpart. This trend may be generalized by the fact that oxygen in a donor destabilizes HOMO, whereas in acceptor would stabilize the HOMO. This indicates that the delicate balance between the donor and acceptor properties in a D–A polymer plays the key role in deciding electronic characteristic of resulting polymers. The LUMO level was estimated relative to the HOMO from the absorption onset values as -3.3 , -3.43 , -3.6 , and -3.02 eV for **P4a**, **P4b**, **P4c**, and **P5**, respectively.

Spectroelectrochemistry

UV–vis absorption spectra of the co-oligomers were recorded in THF solvent (Fig. 2). In all the cases, two absorption bands were found. The λ_{max} corresponds to the higher energy band for **4a**, **4b**, and **4c** is less than 300 nm; but for **5** only, it is 314 nm due to increase in conjugation. The lower energy absorption band of **5** (470 nm) is significantly red shifted than that of **4a** (444 nm), **4b** (441 nm),

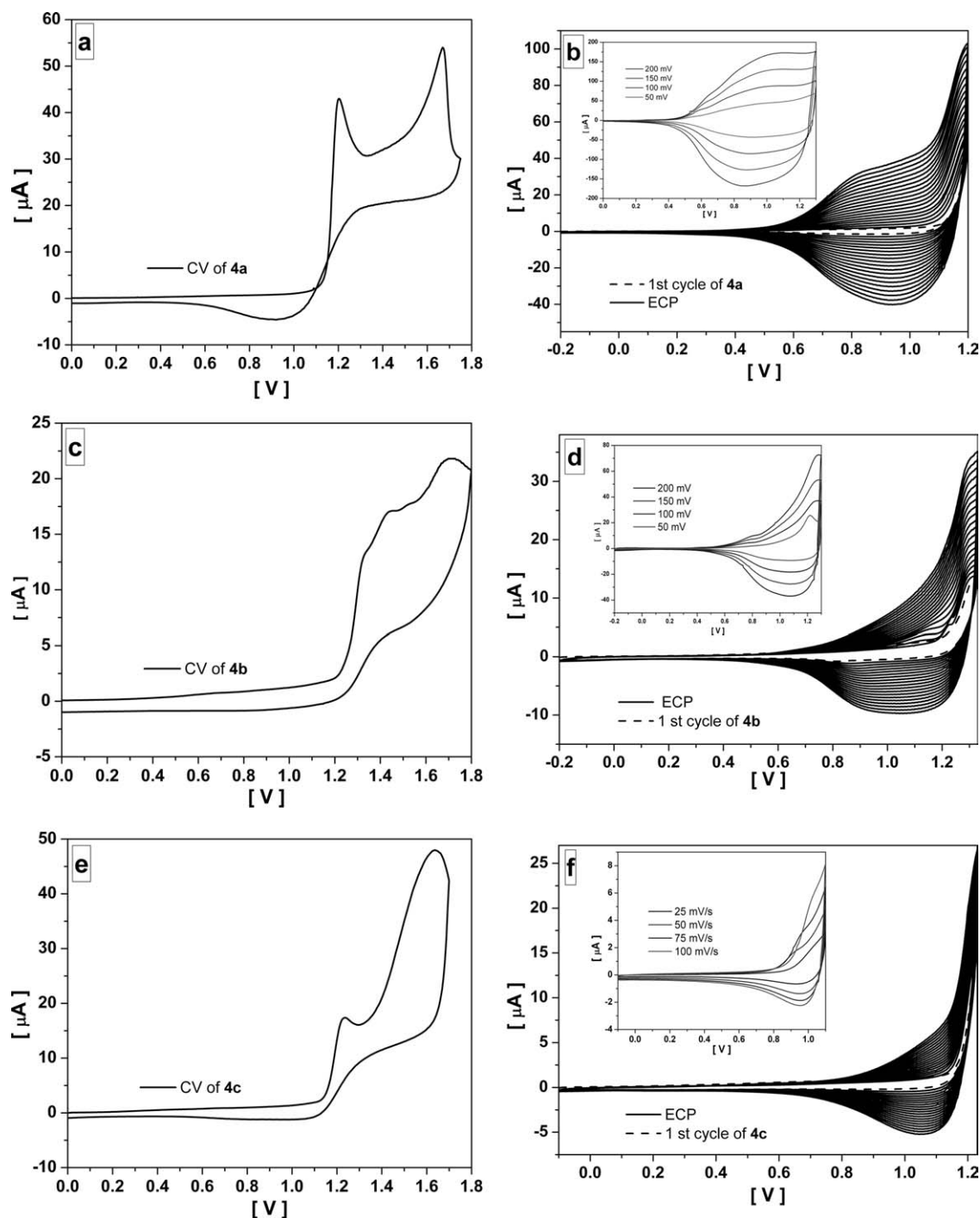


FIGURE 1 CV of **4a** (a), **4b** (c), **4c** (e), and **5** (g) in DCM and Bu_4NClO_4 (TBAPC) on a Pt electrode at a scan rate of 50 mV/s versus Ag/AgCl wire. Multisweep electrochemical polymerization (ECP) of **4a** (b), **4b** (d), **4c** (f), and **5** (h) on a Pt electrode in DCM and 0.1 M TBAPC at 50 mV/s versus Ag/AgCl wire. (Inset) CV of D–A copolymers **P4a** (b), **P4b** (d), **P4c** (f), and **P5** (h) produced in DCM and 0.1 M TBAPC as a function of scan rate.

and **4c** (450 nm). It is in the order of the calculated dipole moment of ground state geometry, which is significantly higher for **5** (8.11 D) than that of **4a** (3.70 D), **4b** (3.39 D), and **4c** (3.24 D).

To find relation between redox processes and UV–vis absorption, polymers **P4a**, **P4b**, **P4c**, and **P5** were chronoamper-

metrically (i.e., the electrode current is recorded over time) deposited on ITO-coated transparent glass electrode, and the spectroelectrochemical properties were investigated. As shown in Figure 3, the absorption spectra in the UV–vis–NIR region of **P4a**, **P4b**, **P4c**, and **P5** films revealed good electrochromic nature at different applied potentials in DCM/TBAPC solvent/electrolyte couple. As seen from the Figure 3, beyond

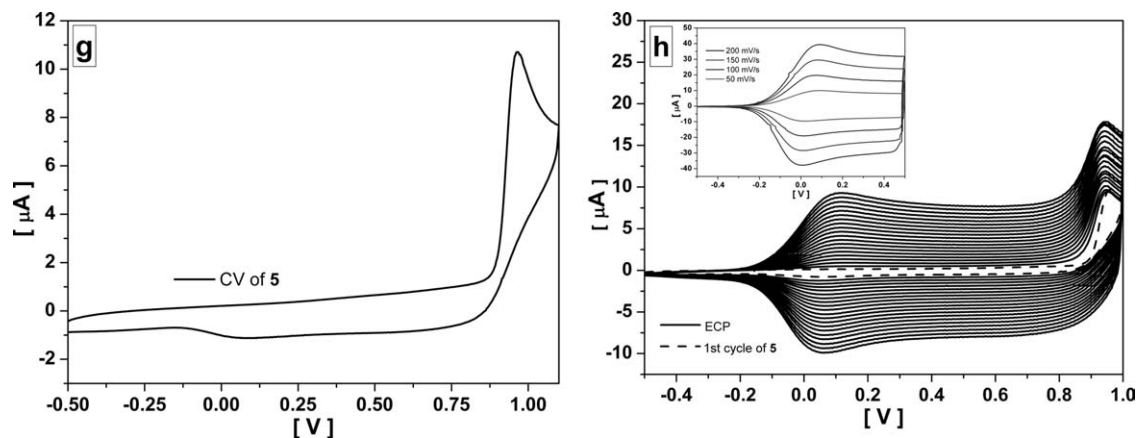


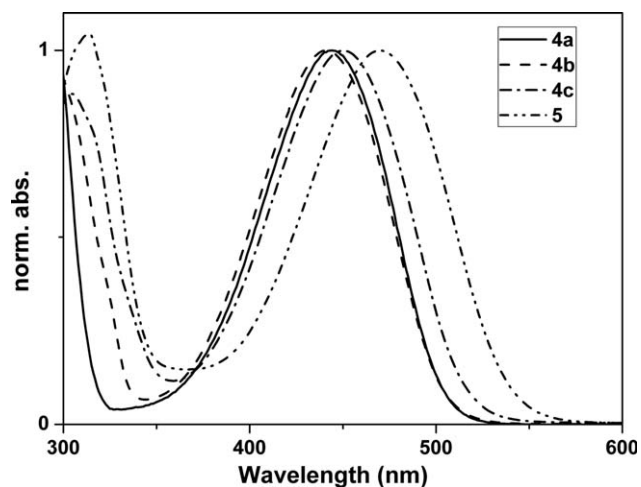
FIGURE 1 Continued

a certain potential (0.8 V for **P4a**, 0.9 V for **P4b**, 1.0 V for **P4c**, and 0.05 V for **P5**), the UV-vis absorption band (arises due to the π - π^* transition of the neutral polymer) started to lose its intensity gradually as the applied potential was increased. Meanwhile, a new absorption band was intensified extending from 700 nm to NIR region owing to the formation of polaron (cation radical). The formation of other charge carriers (bipolaron band) was not observed upon further oxidation for **P4a**, **P4b**, and **P4c**, which could be attributed to the strong electron-accepting nature of BDO that does not allow withdrawal of further electron from the resulting polaronic structures. **P5** revealed two well-separated absorption maxima at 406 nm and 746 nm, which are indispensable for green color to be observed. Upon oxidation, the intensities of the two π - π^* transition bands of **P5** were depleted simultaneously, and formations of two new bands at 960 and 1400 nm indicate the formations of polarons and bipolarons, respectively, which is accompanied by a color change from green to transparent light blue. Replacement of more electron-rich systems like EDOT with furan/thiophene/selenophene afforded polymers with high oxidative stability. The optical band gaps (E_g) were obtained from absorption onsets of the polymer film spectra (onset value) as 1.66 eV (**P4a**, 746 nm), 1.62 eV (**P4b**, 765 nm), 1.59 eV (**P4c**, 779 nm), and 1.25 eV (**P5**, 992 nm), which indicate that the band gap of D-A-D type copolymer can nicely be tuned by only replacing the donor in a polymer backbone. The smaller band gap of the D-A polymer based on EDOT-capped BDS²⁵ compared to that based on EDOT-capped BDO may be rationalized by the degree of bond length alternation (E-N bond, E = O, S, Se) in the benzene ring that increases in the order O < S < Se trending toward a decrease in aromaticity, which affects the conjugation between donor and acceptor unit resulting in destabilization of the HOMO and stabilization of the LUMO.⁴⁰ Low band gap material (to harness more solar photon) with low lying HOMO level (to prevent aerial oxidation) is the prerequisite for an efficient organic photovoltaic devices. EDOT containing polymers generally possess low band gap but high HOMO level, which hampered their application as a light-absorbing donor in organic solar cells. This strategy can be extended to prepare the polymers in which the frontier orbital energy levels

can be tuned with the energy levels of the acceptor such as fullerene to improve the performance of the photovoltaic devices.

Density Functional Theory Calculations

The density functional theory (DFT) using periodic boundary condition (PBC) with B3LYP functional and the 6-31G(d) basis set is applied to determine the geometric and electronic structures and the corresponding energies of HOMO, LUMO, and band gap. The PBC-DFT method, implemented in the Gaussian 03 program package,⁴¹ is a reliable method for predicting the energy gaps of D-A copolymers.⁴² The BDO substituent as an acceptor between two donor units (furan, thiophene, selenophene, or EDOT) of the resulting polymer does not create any geometrical twist in the polymer backbone, which results in uninterrupted π -conjugation along polymer chain that results into small to low band gap polymers. The optimized planar (side view) D-A copolymer backbone is shown in Table 1. The calculated HOMO levels for **P4a**, **P4b**, **P4c**, and **P5** at $k = 0$ are -4.75, -4.92, -4.87, and -4.12 eV, respectively. The theoretical band gaps are as 1.66, 1.62, 1.51, and 1.44 eV, which are in good agreement with the optical band gap.

FIGURE 2 Normalized absorption spectra of co-oligomers **4a**–**4c** and **5** recorded in THF solution.

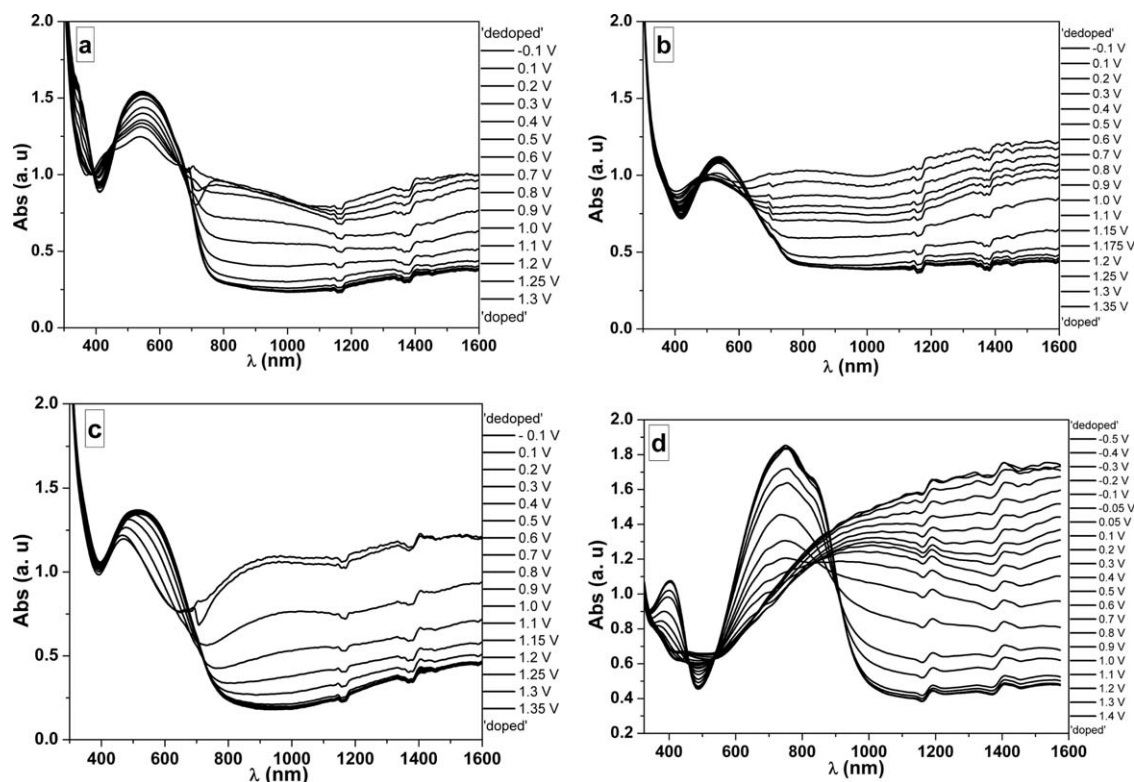
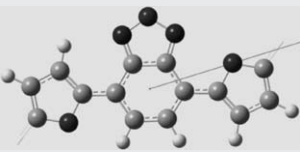
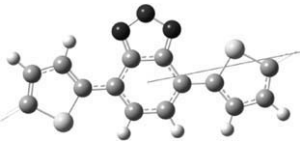
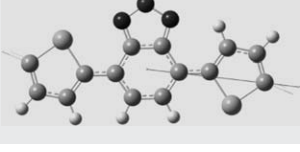


FIGURE 3 Spectroelectrochemistry of **P4a** (a), **P4b** (b), **P4c** (c), and **P5** (d) thin film, prepared on ITO-coated glass slides, as a function of various applied potentials in co-oligomer-free DCM/TBAPC solvent/electrolyte couple.

Theoretically, we found that the HOMO of selenium (**P4c**) or thiophene (**P4b**) based system is more stabilized by 0.12–0.17 eV than their oxygen counterpart (**P4a**) that is in agree-

ment with our experimental observations but contradicts the fact that HOMO of furan containing polymers is more stabilized than their sulfur or selenium analogs.

TABLE 1 Optimized Geometry of the D–A Copolymers at DFT-PBC/B3LYP/6-31G(d)

Polymer	Front View	Side View	HOCO (eV)	LUCO (eV)
P4a			–4.75	–3.09
P4b			–4.92	–3.30
P4c			–4.87	–3.36
P5			–4.12	–2.68

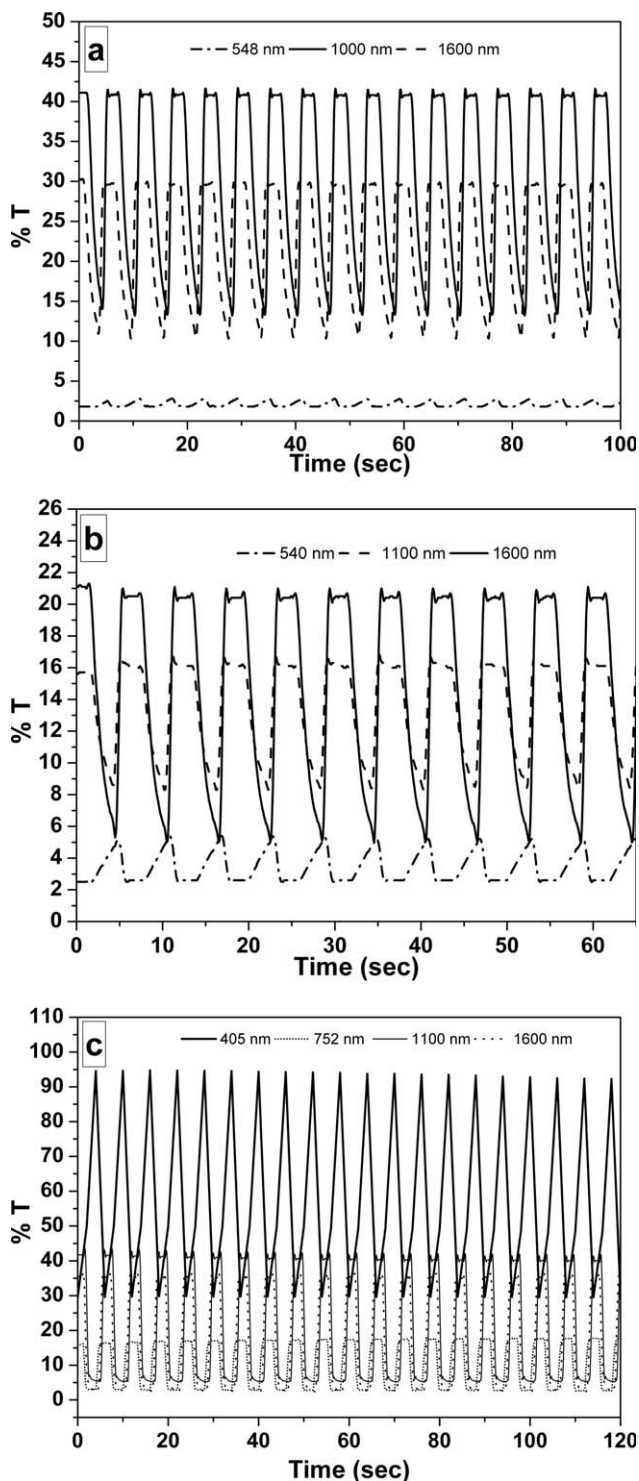


FIGURE 4 Percent transmittance changes of polymer films **P4a** (a), **P4b** (b), and **P5** (c) in monomer-free 0.1 M TBAPC/DCM solution at visible and NIR region.

Chronoabsorptometry

Switching properties of the ITO-coated polymers were investigated by chronoamperometry to monitor the changes in transmittance as a function of time while sweeping the potentials between neutral and fully oxidized states at local

absorption maxima (Fig. 4). As illustrated in Figure 4, **P4a**, **P4b**, and **P5** were switched between oxidized and reduced states with a switching interval of 3 s in a 0.1 M DCM/TBAPC solvent/electrolyte system while measuring their transmittance at their respective absorption maxima (visible region) and NIR region. The contrast was given as the difference between %T in the reduced and oxidized states and reported as $\Delta\%T$. **P4a** and **P4b** show quite similar performance, where 19% (**P4a**) and 16% (**P4b**) of the transmittance modulation are maintained at 1600 nm when the time of the applied potential is switched between -0.1 and $+1.3$ V at 3-s interval. At a similar condition, **P4a** revealed 29% optical contrast at 1000 nm and **P4b** revealed only 8% at 1100 nm. However, their performance was poor near their wavelength maximum even **P4c** also failed to perform better (see Supporting Information). To evaluate the electrochromic properties of **P5**, the **P5** polymer film was electrodeposited onto ITO-coated glass having dimensions of 3×0.7 cm² at a constant potential of 0.95 V versus Ag/AgCl and passing charge of 50 mC. While the films were switched between -0.5 and $+1.3$ V, the percentage transmittance at visible absorption maxima and NIR regions were simultaneously monitored as a function of time (Fig. 4). The **P5** films showed 95% transmittance at the oxidized and a 29% transmittance at the neutral state with a rapid switching time of less than 2 s and noteworthy optical contrast of 66% at 405 nm (the first π - π^* transition), which is undoubtedly higher than analogous BDT and BDS based green D-A copolymers. The optical contrast for **P5** near λ_{\max} (750 nm, the second π - π^* transition) was calculated as 14% with a switching time of 0.9 s. In NIR region, polymer **P5** showed 36% (1100 nm) to 34% (1600 nm) transmittance change in less than 1 s. The coloration efficiency of the **P5** film was found to be 101 cm² C⁻¹ for 405 nm. **P4a**, **P4b**, and **P4c** exhibited lower optical contrast values in visible region compared to **P5** due to their extant absorption at around 400–600 nm.

CONCLUSIONS

A new series of D-A-D polymers, comprising the least explored BDO unit as acceptor, have been synthesized and characterized electrochemically. Our experimental investigations indicated that BDO has the highest electron-acceptance property than its sulfur, nitrogen, or selenium counterpart, as incorporation of acceptor like BDO has affected each co-oligomer's oxidation potential and thus the oxidative stability. However, it is not always necessary that HOMO of oxygen containing polymers would stabilize more as inclusion of oxygen (as BDO unit) instead of sulfur or selenium has affected each co-oligomer in a different way. As a result, **4a** oxidizes at almost same potential where its selenium counterpart does, which might be credited to the more extended conjugation. The EDOT-BDO based polymer **P5** films exhibit better electrochromic property compared to other BDO-based copolymers with a high contrast ratio (66%) and moderate coloration efficiency at 405 nm. The combination of furan and BDO can make an important contribution in producing environmentally sustainable organic electronic materials.

ACKNOWLEDGMENTS

BPB thanks UGC for his fellowship and SSZ thanks DRDO, India for funding.

REFERENCES AND NOTES

- 1 Perepichka, I. F.; Perepichka, D. F. *Handbook of Thiophene-Based Materials: Applications in Organic Electronics and Photonics*; Wiley: New York, **2009**.
- 2 Groenendaal, L.; Jonas, F.; Freitag, D.; Pielartzik, H.; Reynolds, J. R. *Adv. Mater.* **2000**, *12*, 481–494.
- 3 Groenendaal, L.; Jotti, G.; Aubert, P.; Waybright, S. M.; Reynolds, J. R. *Adv. Mater.* **2003**, *15*, 855–879.
- 4 Roncali, J.; Blanchard, P.; Frere, P. *J. Mater. Chem.* **2005**, *15*, 1589–1610.
- 5 Spencer, H. J.; Skabara, P. J.; Giles, M.; McCulloch, I.; Coles, S. J.; Hursthouse, M. B. *J. Mater. Chem.* **2005**, *15*, 4783–4792.
- 6 Patra, A.; Bendikov, M. *J. Mater. Chem.* **2010**, *20*, 422–433.
- 7 Patra, A.; Wijsboom, Y. H.; Zade, S. S.; Li, M.; Sheynin, Y.; Leitus, G.; Bendikov, M. *J. Am. Chem. Soc.* **2008**, *130*, 6734–6736.
- 8 Shahid, M.; McCarthy-Ward, T.; Labram, J.; Rossbauer, S.; Domingo, E. B.; Watkins, S. E.; Stingelin, N.; Anthopoulos, D. D.; Heeney, M. *Chem. Sci.* **2012**, *3*, 181–185.
- 9 Mohammed, A.-H.; Mohammed, A. B.; Florian, C.; Scott, E. W.; Thomas, D. A.; Natalie, S.; Heeney, M. *Macromolecules* **2011**, *44*, 5194–5199.
- 10 Chung, D. S.; Kong, H.; Yun, W. M.; Cha, H.; Shim, H.-K.; Kim, Y.-H.; Park, C. E. *Org. Electron.* **2010**, *11*, 899–904.
- 11 Haid, S.; Mishra, A.; Uhrich, C.; Pfeiffer, M.; Bäuerle, P. *Chem. Mater.* **2011**, *23*, 4435–4444.
- 12 Das, S.; Zade, S. S. *Chem. Commun.* **2010**, *46*, 1168–1170.
- 13 Das, S.; Bedi, A.; Krishna, G. R.; Reddy, C. M.; Zade, S. S. *Org. Biomol. Chem.* **2011**, *9*, 6963–6972.
- 14 Das, S.; Dutta, P. K.; Panda, S.; Zade, S. S. *J. Org. Chem.* **2010**, *75*, 4868–4871.
- 15 Glenis, S.; Benz, M.; LeGoff, E.; Schindler, J. L.; Kannewurf, C. R.; Kanatzidis, M. G. *J. Am. Chem. Soc.* **1993**, *115*, 12519–12525.
- 16 Gidron, O.; Diskin-Posner, Y.; Bendikov, M. *J. Am. Chem. Soc.* **2010**, *132*, 2148–2150.
- 17 Gidron, O.; Dadvand, A.; Sheynin, Y.; Bendikov, M.; Perepichka, D. F. *Chem. Commun.* **2011**, *47*, 1976–1978.
- 18 Beaujuge, P. M.; Holcombe, T. W.; Lee, O. P.; Fréchet, J. M. J. *J. Am. Chem. Soc.* **2010**, *132*, 15547–15549.
- 19 Wang, X.; Chen, S.; Sun, Y.; Zhang, M.; Li, Y.; Li, X.; Wang, H. *Polym. Chem.* **2011**, *2*, 2872–2877.
- 20 Gandini, A. *Macromolecules* **2008**, *41*, 9491–9504.
- 21 Binder, J. B.; Ronald, R. T. *J. Am. Chem. Soc.* **2009**, *131*, 1979–1985.
- 22 Havinga, E. E.; Ten-Hoeve, W.; Wynberg, H. *Polym. Bull.* **1992**, *29*, 119–126.
- 23 Roncali, J. *Chem. Rev.* **1997**, *97*, 173–205.
- 24 Durmus, A.; Gunbas, G. E.; Camurlu, P.; Toppare, L. *Chem. Commun.* **2007**, 3246–3248.
- 25 Cihaner, A.; Algi, F. *Adv. Funct. Mater.* **2008**, *18*, 3583–3589.
- 26 Lu, N. A. O.; Balan, A.; Baran, D.; Cirpan, A.; Toppare, L. *J. Polym. Sci. Part A: Polym. Chem.* **2010**, *48*, 5603–5610.
- 27 Caputo, B. J. A.; Welch, G. C.; Kamkar, D. A.; Henson, Z. B.; Nguyen, T.-Q.; Bazan, G. C. *Small* **2011**, *7*, 1422–1426.
- 28 Jiang, J.-M.; Yang, P.-A.; Chen, H.-C.; Wei, K.-H. *Chem. Commun.* **2011**, *47*, 8877–8879.
- 29 Ding, P.; Zhong, C.; Zou, Y.; Pan, C.; Wu, H.; Cao, Y. *J. Phys. Chem. C* **2011**, *115*, 16211–16219.
- 30 Blouin, N.; Michaud, A.; Gendron, D.; Wakim, S.; Blair, E.; Plesu, R. N.; Durocher, G.; Tao, Y.; Leclerc, M. *J. Am. Chem. Soc.* **2008**, *130*, 732–742.
- 31 During our research work on the manuscript, Cihaner et al. have reported compound **4b** and **5** and their electropolymerization. İçli-Özkut, M.; Algi, M. P.; Ötaz, Z.; Algi, F.; Önal, A. M.; Cihaner, A. *Macromolecules* **2012**, *45*, 729.
- 32 Liebeskind, L. S.; Wang, J. *Tetrahedron* **1993**, *49*, 5461–5470.
- 33 Manuela, M.; Raposo, M.; Mauricio, A.; Fonseca, C.; Kirsch, G. *Tetrahedron* **2004**, *60*, 4071–4178.
- 34 Udum, Y. A.; Tarkuc, S.; Toppare, L. *Synth. Met.* **2009**, *159*, 361–365.
- 35 Turbiez, M.; Frère, P.; Allain, M.; Vidolot, C.; Ackermann, J.; Roncali, J. *Chem. Eur. J.* **2005**, *11*, 3742–3752.
- 36 Zarei, A.; Hajipour, A. R.; Khazdooz, L.; Aghaei, H. *Tetrahedron Lett.* **2009**, *50*, 4443–4445.
- 37 Deghati, P. Y. F.; Borghini, A.; Nieuwendijk, A. M. C. H.; Groote, M. D.; Jzerman, A. P. I. *Bioorg. Med. Chem.* **2003**, *11*, 899–908.
- 38 Blouin, N.; Michaud, A.; Gendron, D.; Wakim, S.; Blair, E.; Neagu-Plesu, R.; Belletete, M.; Durocher, G.; Tao, Y.; Leclerc, M. *J. Am. Chem. Soc.* **2008**, *130*, 732–742.
- 39 Experimental HOMO = $-e(E_{\text{onset}}^{\text{ox}} - E_{1/2}^{\text{ferrocene}} + 4.8)$ (eV).
- 40 Gibson, G. L.; Mc-Cormick, T. M.; Seferos, D. S. *J. Am. Chem. Soc.* **2012**, *134*, 539–547.
- 41 Frisch, M. J.; Trucks, G. W.; Schlegel, H. B.; Scuseria, G. E.; Robb, M. A.; Cheeseman, J. R.; Scalmani, G.; Barone, V.; Mennucci, B.; Petersson, G. A.; Nakatsuji, H.; Caricato, M.; Li, X.; Hratchian, H. P.; Izmaylov, A. F.; Bloino, J.; Zheng, G.; Sonnenberg, J. L.; Hada, M.; Ehara, M.; Toyota, K.; Fukuda, R.; Hasegawa, J.; Ishida, M.; Nakajima, T.; Honda, Y.; Kitao, O.; Nakai, H.; Vreven, T.; Montgomery, J. A., Jr.; Peralta, J. E.; Ogliaro, F.; Bearpark, M.; Heyd, J. J.; Brothers, E.; Kudin, K. N.; Staroverov, V. N.; Kobayashi, R.; Normand, J.; Raghavachari, K.; Rendell, A.; Burant, J. C.; Iyengar, S. S.; Tomasi, J.; Cossi, M.; Rega, N.; Millam, J. M.; Klene, M.; Knox, J. E.; Cross, J. B.; Bakken, V.; Adamo, C.; Jaramillo, J.; Gomperts, R.; Stratmann, R. E.; Yazyev, O.; Austin, A. J.; Cammi, R.; Pomelli, C.; Ochterski, J. W.; Martin, R. L.; Morokuma, K.; Zakrzewski, V. G.; Voth, G. A.; Salvador, P.; Dannenberg, J. J.; Dapprich, S.; Daniels, A. D.; Farkas, O.; Foresman, J. B.; Ortiz, J. V.; Cioslowski, J.; Fox, D. J. *Gaussian 09, Revision A.02*; Gaussian, Inc.: Wallingford CT, **2009**.
- 42 Pappenfus, T. M.; Schmidt, J. A.; Koehn, R. E.; Alia, J. D. *Macromolecules* **2011**, *44*, 2354–2357.